Originalarbeit

Berg Huettenmaenn Monatsh (2025) Vol. 170 (3): 148–157
https://doi.org/10.1007/s00501-025-01561-0
© The Author(s) 2025

BHM Berg- und Hüttenmännische Monatshefte

Investigation of Design Potentials for Welding PBF-LB/M Manufactured Pure Copper Busbars to Conventional Copper Conductors

Carsten Putz, Tim Grundmann, and Johannes Henrich Schleifenbaum

DAP, RWTH Aachen University, Aachen, Germany

Received December 19, 2024; accepted February 4, 2025; published online February 26, 2025

Abstract: The advantages of the laser beam powder bed fusion process for metals (PBF-LB/M), such as geometric complexity due to increased design freedom or function integration, offer a great potential for optimizing products in the automotive sector. However, it often does not go beyond prototyping and small series as productivity is too low for the required quantities and economies of scale can rarely be exploited lucratively. In the field of e-mobility, hairpin technology has recently come to dominate the copper winding of traction drives. The research field of additive manufacturing (AM) of copper windings for e-machines has made significant progress in recent years, but additive manufacturing has not yet prevailed over conventional technologies, despite the product advantages.

In this study the approach of transferring the complexity of conventional hairpin windings into additively manufactured busbar assemblies and then joining them to conventional windings using laser welding is investigated. The advantage is that the less complex components of an electric machine can still be manufactured conventionally with high productivity.

For this purpose, different design variants of the connection geometry are developed at the interconnection area of the busbars and manufactured from copper using PBF-LB/M. The manufactured design variants are then joined to the conventional copper conductors using a laser welding process. A comprehensive analysis and evaluation of the connections is then carried out in four main categories. The design, the electrical conductivity, the critical heating und real boundary conditions as well as and the weldability are examined. Three designs with promising results and requirement fulfilling properties were identified. The results show that functions like form fitting can directly be added to the AM parts and by the complexity transfer, both advantages of additive manufacturing and conventional manufacturing can be combined by means of laser welding.

Keywords: Laser welding, Laser powder bed fusion, PBF-LB/M, Pure copper, E-mobility, Hairpin, Winding, E-motor, E-machine

Untersuchung von Designpotentialen für das Verschweißen von PBF-LB/M-gefertigten Reinkupfer-Stromschienen mit konventionellen Kupferleitern

Zusammenfassung: Die Vorteile des Laserstrahl-Pulverbettschmelzverfahrens für Metalle (PBF-LB/M), wie z. B. geometrische Komplexität durch erhöhte Designfreiheit oder Funktionsintegration, bieten ein großes Potenzial zur Optimierung von Produkten im Automobilbereich. Allerdings geht es oft nicht über Prototypen und Kleinserien hinaus, da die Produktivität für die benötigten Stückzahlen zu gering ist und Skaleneffekte selten lukrativ genutzt werden können. Im Bereich der E-Mobilität dominiert im letzten Jahrzehnt die Hairpin-Technik bei der Kupferwicklung von elektrischen Traktionsantrieben. Das Forschungsfeld der additiven Fertigung (AM) von Kupferwicklungen für E-Maschinen hat in den letzten Jahren deutliche Fortschritte gemacht, jedoch hat sich die additive Fertigung trotz der Produktvorteile noch nicht gegenüber konventionellen Technologien durchgesetzt.

In dieser Studie wird daher der Ansatz untersucht, die Komplexität konventioneller Hairpin-Wicklungen in additiv gefertigte Stromschienen-Baugruppen zu übertragen und diese dann mittels Laserschweißen mit konventionellen Wicklungen zu verbinden. Der Vorteil ist, dass die weniger komplexen Komponenten einer elektrischen Maschine weiterhin mit hoher Produktivität konventionell gefertigt werden können.

C. Putz, M.Sc. (✉)
DAP,
RWTH Aachen University,
Campus-Boulevard 30,
52074 Aachen, Germany
carsten.putz@dap.rwth-aachen.de

Dazu werden verschiedene Designvarianten der Anschlussgeometrie im Verbindungsbereich der Stromschienen entwickelt und mit PBF-LB/M aus Kupfer gefertigt. Die gefertigten Designvarianten werden dann mit konventionellen Kupferleitern mittels eines Laserschweißverfahrens verbunden. Anschließend wird eine umfassende Analyse und Bewertung der Verbindungen in vier Hauptkategorien durchgeführt. Hierbei werden das Design, die elektrische Leitfähigkeit, die kritische Erwärmung unter realen Randbedingungen sowie die Schweißbarkeit untersucht. Es wurden drei Designs mit vielversprechenden Ergebnissen und anforderungsgerechten Eigenschaften identifiziert. Die Ergebnisse zeigen, dass Funktionen wie Formschlüsse direkt in die AM-Bauteile eingebracht werden können und durch den Komplexitätstransfer die Vorteile der additiven Fertigung und der konventionellen Fertigung mittels Laserschweißen kombiniert werden können.

Schlüsselwörter: Laserschweißen, Laser Powder Bed Fusion, PBF-LB/M, Reinkupfer, E-Mobilität, Hairpin, Wicklung, E-Motor, E-Maschine, Additive Fertigung

1. Introduction

The laser beam powder bed fusion process for metals (PBF-LB/M) offers the possibility of realizing very complex geometries and integrating functions into components. In addition, the processing of pure copper using PBF-LB/M has been thoroughly researched and further developed over the last few years, especially in the application for electrical conductors. It therefore makes sense to realize copper windings using PBF-LB/M in the field of electric traction drives. The design of the copper winding can be very complex. For this reason, initial approaches already exist to manufacture the complex winding using additive manufacturing (AM) processes directly or in hybrid processes (see Fig. 1; [1–3]). However, as the productivity of the manufacturing process is very low, applications in the automotive sector rarely go beyond prototypes or very small series. For this reason, the approach of transferring the complexity of the winding design to an external stator assembly, manufacturing it using the PBF-LB/M process and then joining it to the conventionally manufactured winding using laser welding is being pursued. [4].

The laser welding process for copper presents similar challenges to processing using the PBF-LB/M process. The degree of absorption of solid copper is very low at around 4% when using laser radiation in the infrared wavelength range [5]. A high energy input is necessary to melt the copper. During the transition to the liquid phase, however, the degree of absorption increases significantly and can reach up to 100% when a vapor capillary is formed [6].

The jump in absorption during the phase change causes a rapid heating of the molten copper and the formation of local hotspots in the weld pool, which often leads to weld defects such as spatter, ejections, and pores [5]. The potential for defects is further increased by the high thermal conductivity of copper and the low viscosity of the molten copper. The surrounding solid base material can dissipate the welding heat very quickly from the weld area, which can lead to excessive heat dissipation. Cooling too quickly can result in distortions, cracks, or gas inclusions [5]. To counteract this, pulsed laser radiation can be used. The adjustment is shown qualitatively in the following figure. This temporal adjustment of the laser power within the individual pulses leads to an increase in process quality [7].

Studies have already been carried out and research has been conducted into the joining of additively manufactured components made from Inconel 718 or AlSi10Mg. However, no process parameters were found on which to base the laser welding of additively manufactured pure copper samples [8–10].

This study therefore investigates the question of which design is best suited for the joining geometry of PBF-LB/M copper conductors to conventional copper conductors using the AM design potentials in order to join them together using laser welding. For this purpose, different AM design variants of the joint geometry are developed, welded to conventional conductors and the welded joints are comprehensively analyzed.

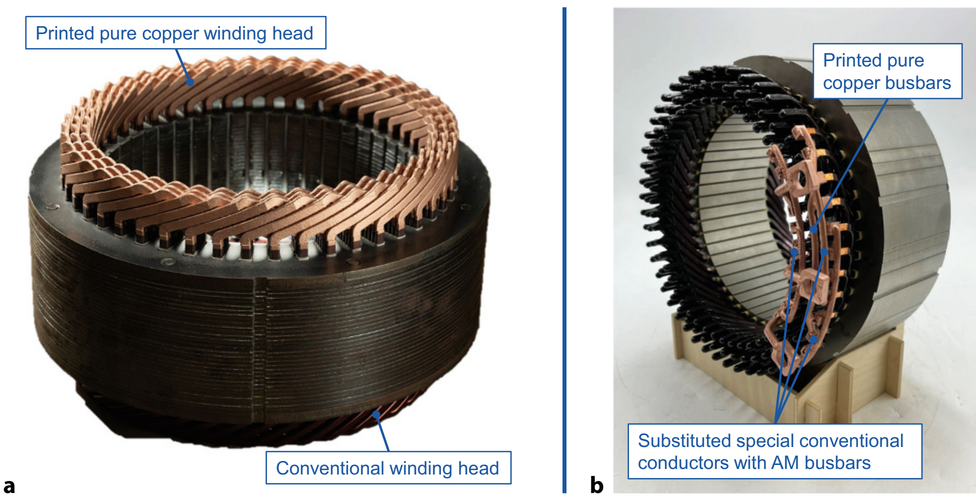

Fig. 1: Hybrid PBF-LB/M of pure copper windings (**a**) [4] | PBF-LB/M printed pure copper busbars [3]

© The Author(s)

2. Methods and Implementation

The overall methodical approach of this study can be seen in Fig. 2. First, methods regarding general product development are used to create the different design variants of interconnections. The different design variants are then additively manufactured from copper in multiple versions using the PBF-LB/M process before they are finally welded to conventional copper conductors using a laser welding process. An initial visual inspection serves as the basis for further design iterations. The developed, additively manufactured, and welded samples are then examined and evaluated with regard to design aspects as well as theelectrical, thermal, and welding quality. The individual approaches and methods of the procedures are described in more detail in the following paragraphs.

PDP and Design The process for creating the design is based on the product development methods according to *Feldhusen* and product development process guidelines. First of all, the basic requirements are defined. Utilizing the potential of the PBF-LB/M process, such as design freedom and functional integration, the design of the interface between the AM conductor and the conventional conductor for the laser welding process is to be created in such a way that a self-supporting weld joint is produced by a form or force fit. In the transition zone, the change of the conductor cross-sectional area should also be kept as small as possible in order to keep the electrical resistance as constant as possible and not create any thermal hotspots. Furthermore, the effective areas of the conventional conductor with the dimensions 4 × 2 mm (width × thickness) must be addressed. The different design variants are derived from various basic concepts for meeting the requirements [11, 12].

To save time and ensure reproducibility, a basic geometry with constant framework conditions is created first (Fig. 3). In order to ensure the same conductor length for measuring the electrical conductivity, the geometry length is set at 70 mm from the end of the PBF-LB/M geometry to the conductor center point. The diameter of the PBF-LB/M geometry is set to 3.2 mm outside the actual connection point. This corresponds to the conductor cross-section of 8 mm^2 of the conductor samples used. Starting from the basic model, 12 geometry variations are then developed. After the first process loop, which includes the design, the PBF-LB/M process and the laser welding process, an iteration process is carried out and a further eight geometry variations are developed. This allows the initial findings from the manufactured samples to be analyzed and interpreted, which can be incorporated into the design development process in the second iteration stage. Any directly identifiable weak points and errors can thus be optimized. The different developed design variants can be seen in Fig. 4.

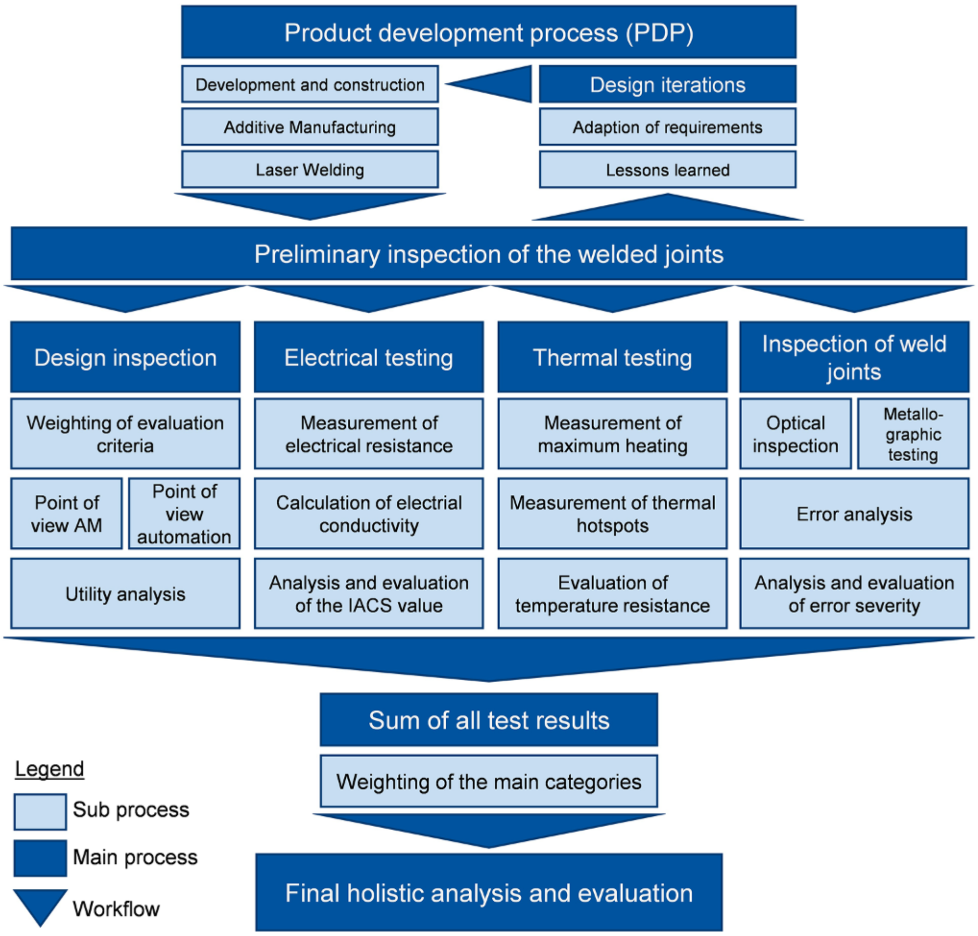

Fig. 2: Overall methodical approach of this study to develop and identify requirement fulfilling design variants

Fig. 3: Basic geometry CAD model for the development of new interface design variants

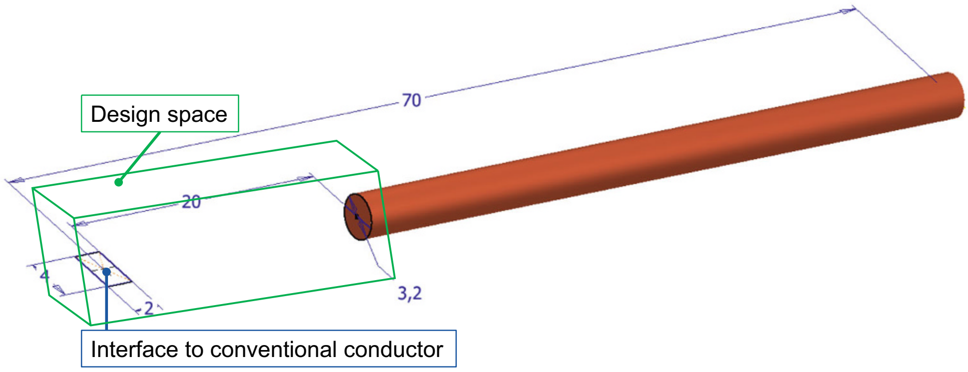

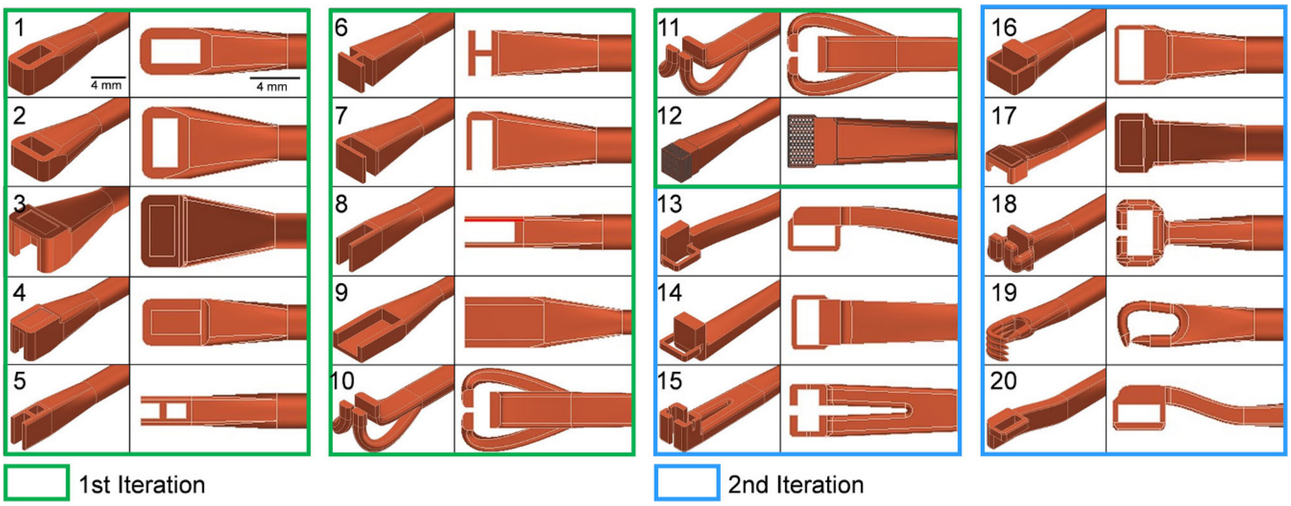

Fig. 4: Developed design variants of the interface geometry for the connection joint to conventional copper wire

PBF-LB/M An EOS M290 system is available for manufacturing the developed design variants. Due to the low absorption rate of the copper powder with a standard Yb fiber laser in the infrared range (1064 nm wavelength, 400 W power), a post-treated copper powder is used for better processability (Fig. 5). A special post-treatment process patented by Infinite Flex® makes it possible to use this copper powder with all common infrared lasers ($\lambda = 1064$ nm) in the PBF-LB/M process [13]. In the post-treatment process, at least 30% of the surface of the particle core is covered by laser absorbers. The laser absorbers are particles of a metal hydroxide, for example dicopper hydroxide phosphate. The degree of absorption of the bonded laser absorbers is at least 20%, preferably 30%, which significantly improves the coupling of the laser's radiation energy. The laser absorbers are bound to the surface of the particle core by adsorption using van der Waals forces [14]. Due to the bonding of the laser absorbers to the surface, the energy is transferred to the particle core by thermal conduction.

The manufacturing of the samples was carried out with the following parameters and the Infinite Flex® copper powder shown in Table 1.

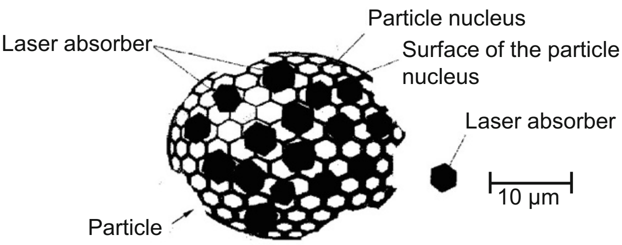

Fig. 5: Post-treated powder particle [14]

Laser Welding A system is available for the laser welding process that is used for welding conventional copper wires in electric motor production. An infrared laser source (1070 nm) is also used here. but with a maximum output of 8 kW and the option of pulsing (continuous wave to 10 kHz). Since a literature search did not produce any promising parameter sets for AM part and conventional part combination, a parameter set of purely conventional copper welding pairings is used as a starting point. The conventional conductors are first cut to length on a Wafios® FMU E CNC bending machine. Afterwards, the electrical insulation layer on the conventional copper wire is removed using a laser. Conventional conductors and printed conductors were then mounted in a welding fixture in order to increase the repeat accuracy of the laser welding process and always create the same boundary conditions (Fig. 6a). Afterwards, the laser welding process was carried out.

© The Author(s)

TABLE 1
Process parameters for the PBF-LB/M process

EOS M290: Yb-Faser-Laser (1064 nm)					Laser			
Description	Designation	Parameter set	Type	Layer thickness [mm]	Power [W]	Speed [mm/s]	Energy density [J/mm²]	Offset [mm]
Part geometry	Solid	Hatch	InFill	0.04	360	430	161	0.13
			UpSkin	0.04	360	650	106.51	0.13
			DownSkin	0.04	360	540	128.21	0.13
		Contour	Std. contour	0.04	360	250	36	0
			Down contour	0.04	360	310	29.03	0
			OnPart contour	0.04	360	250	36	0
Wall support	Solid support	Hatch	InFill	0.04	360	430	161	0
			UpSkin	0.04	360	650	106.51	0
			DownSkin	0.04	360	540	128.21	0
		Contour	Std. contour	0.04	360	250	36	0
			Down contour	0.04	360	310	29.03	0
			OnPart contour	0.04	360	450	36	0
Inner support	Non solid support	Support	Support	0.08	360	430	10.47	0

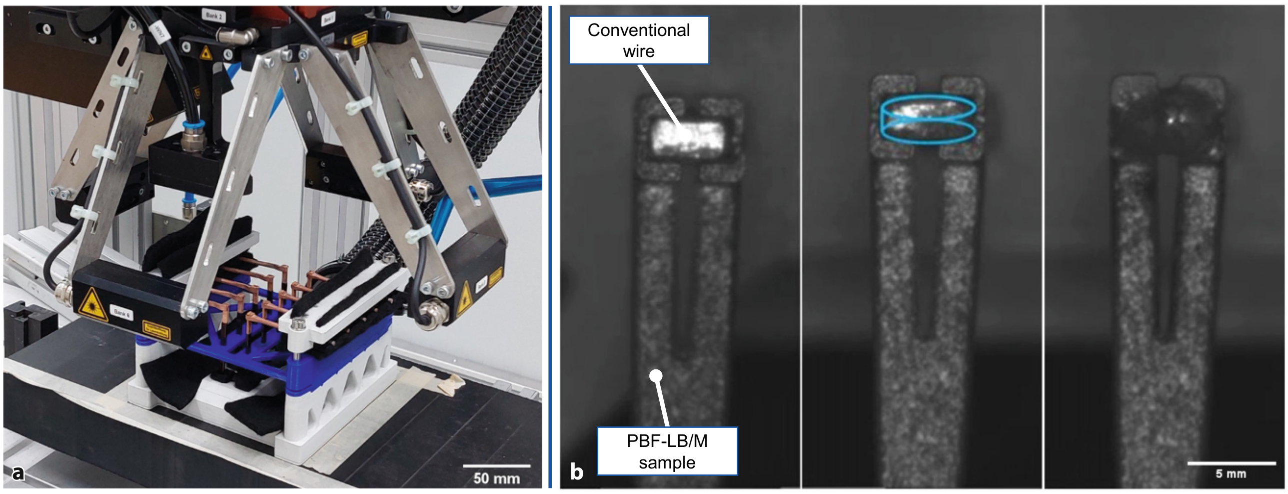

Fig. 6: Welding fixture with mounted samples (**a**) | Welding process steps of a single sample (**b**)

Table 2 shows the used parameter set for the laser welding process.

Design Analysis and Evaluation When analyzing the developed design variants of the connection geometries, the individual designs are evaluated with regard to ten different criteria. There are five evaluation levels (0–4, not at all fulfilled—completely fulfilled) [15]. The evaluation criteria are as follows: Utilization of PBF-LB/M potentials such as function integration or design freedom; design features to realize a form and/or force fit to eliminate additional necessary clamping tools for the welding process; automation capability, which means how the new design can be adapted in existing conventional production lines without additional adjustments; complexity, which will be directly quantified by calculating the ratio of amount of triangles due to tessellation and surface area; material efficiency, quantified by the design volume; space requirement, quantified by the necessary dimensions around the interface of the conventional conductor; expandability, which means openness for further interfaces; production time; robustness and functional fulfillment. The individual criteria are also weighted against each other in a pairwise comparison. On the one hand, there is the view of optimal utilization of the potential of AM and, on the other hand, the view of optimal automation for industrialization. Finally, two utility value analyses of the design variants are carried out using the evaluation levels and the weightings of the two perspectives.

TABLE 2
Laser welding process parameters

Laser power [kW]	Scan speed [mm/s]	Welding track shape	Repetitions
3	700	Double ellipse	4× top ellipse, 3× bottom ellipse, 1× top ellipse

 © The Author(s)

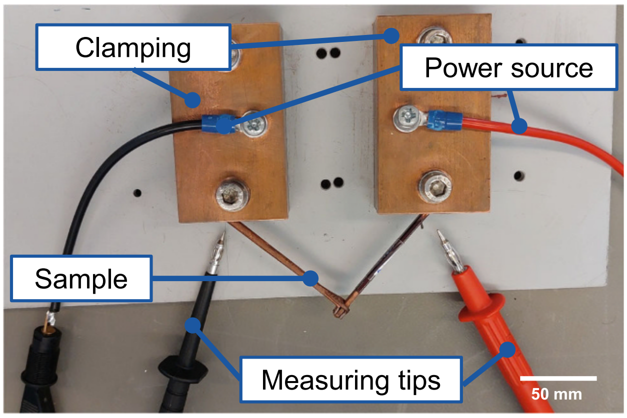

Fig. 7: Setup of the electrical resistance measurement

Electrical Analysis and Evaluation A four-wire resistance measurement is carried out according to *Mühl* [16], also known as the Kelvin or four-wire method. This is a technique for precisely measuring the electrical resistance of a component. This type of measurement avoids the inaccuracies caused by the resistance of the connecting leads used in the measurement. Four separate connections are made to the component to be measured. A current with a constant and known amperage $I_0 = 10$ A is fed into the component via two of the connections. This is done via a precision current source with an output fluctuation <0.01% and a confidence interval >99%. This means that no measurement inaccuracies are introduced by the current source. The confidence interval describes the probability that the output fluctuation lies within the specified interval [17]. The two other connections are used to measure the voltage drop across the component under test. In this work, a measurement accuracy of 1 µV is aimed for.

In this contribution, a FLUKE® 5500 A calibrator is used as a voltage source with a maximum DC deviation of 0.01% and a confidence interval of over >99%. An HP® 3458 A digital multimeter with a measurement resolution of 8.5 digits and a transmission accuracy of 0.0008% is used to measure the very small resistance differences in the different geometries. The test setup is shown in Fig. 7. This process is repeated for all geometries.

Following the four-wire measurement, the electrical resistance R_{jk} of the connection geometries is calculated from the set constant current I_0 and the measured voltage U_{jk}. The index *j* denotes the consecutive numbering of the design variant and *k* the sample number of the variant: $R_{jk}= U_{jk}/I_0$. The electrical conductivityσ σ_{jk} is calculated for each variant using the calculated resistance R_{jk}, the measured conductor length l_{jk} and the conductor cross-section *A*, which is assumed to be constant as $A = 8\,\text{mm}^2$: $\sigma_{jk}= l_{jk}/(A * R_{jk})$. A mean value of the electrical conductivity $\sigma_{j\,m}$ and the standard deviation are then calculated from the five identical samples. The IACS value for each variant is calculated from the mean values of the electrical conductivities. The International Annealed Copper Standard (IACS) value is an empirical standard created in 1914 to evaluate the electrical conductivity of copper [18]. An IACS value of 100% is defined by the electrical conductivity of pure copper at 20 °C: σ_0 (20 °C) = 58 * 10^6 S/m.

The IACS value is given as a percentage for each design variant: $\text{IACS}_j= \sigma_{j\,m}/\sigma_0$.

In addition, two geometries manufactured entirely by PBF-LB/M and two conventional conductors with identical conductor lengths are measured. These additional measurements are used to compare and classify the measured values.

Thermal Analysis and Evaluation The third main category for evaluating the joint geometries is the thermal evaluation. The maximum heating of the joint geometries at a constant current $I_T = 200$ A is investigated to recreate temperature levels that will appear under real application usage. The maximum heating is measured at a fixed time interval of thirty seconds, starting after a warm-up phase of one minute. A sensor is placed on the welded joint to measure the temperature (Fig. 8a). The lower the maximum measured temperature in the specified time period, the better.

For thermal testing, the geometries to be tested are clamped between two copper holders to which a voltage source is connected. An EA-PS® 8080-250 with a maximum current of $I = 250$ A is used as the voltage source for the measurement. The temperature measurement is carried out with an Extech Industries® TM300 Dual *K/J* thermal sensor. The sensor used has an accuracy of 0.1 °C. Additionally, thermal hotspots are then examined using a FLIR® E8 thermal imaging camera. The joint geometries *j* are not allowed to heat up critically ($T_j < T_{crit}$) under these conditions, as otherwise the insulation of the copper conductors could be damaged. The insulation of the conductors is classified according to *DIN 60085* in insulation

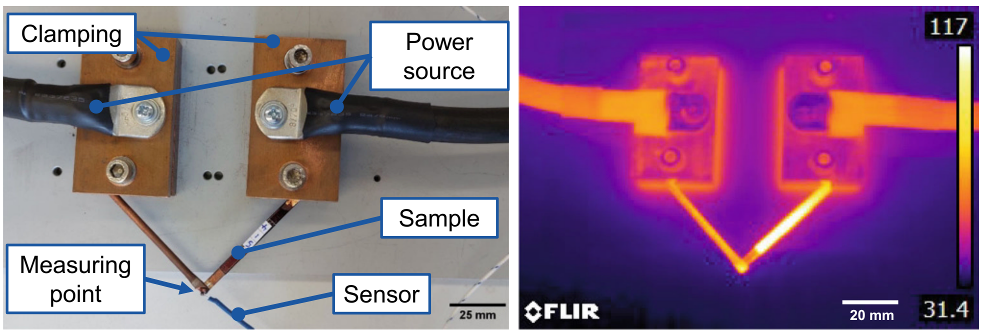

a b

Fig. 8: Setup of the temperature measurement (**a**) | Thermal image of a welded sample under constant current (**b**)

© The Author(s)

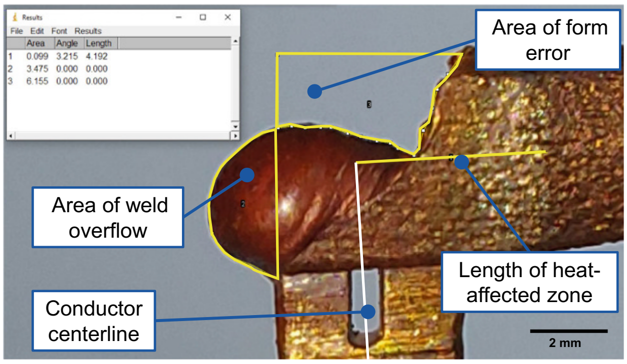

Fig. 9: Screenshot of a measured weld joint using ImageJ®

class, which specifies a melting or destruction temperature in continuous operation of $T_{crit} < 180\,°C$ [19]. A conductor manufactured entirely from PBF-LB/M with the same conductor cross-sections is also measured as a comparison. This process is repeated for all geometries.

Inspection and Evaluation of Weld Joints First, a non-destructive visual inspection is carried out by using ImageJ® measuring software (Fig. 9). For this purpose, high-resolution photographs are taken in three positions (isometric, top view, side view) of all connection geometries. The software's measuring scale is then first calibrated using a known measuring distance. The known conductor cross-sections of the conductor samples are used for the calibration. The measuring distances can be converted from pixels to millimetres by the software. The process is shown as an example for connection geometry 5 in the figure. Defects and irregularities visible from the outside are examined in accordance with *DIN 5817* in the categories of *DIN 6520-1*. For the visual inspection, shape defects (ordinal number 500), discoloration of the copper color in the the heat-affected zone (ordinal number 6101) and weld metal overflows (ordinal number 506) are examined and evaluated in accordance with *DIN 6520-1* [20, 21]. For the shape defects, the ratio of the weld zone to the original height or width of the PBF-LB/M geometries and conductor samples is compared. Too large a change in shape can have considerable negative consequences for the joint strength and electrical conductivity.

In the heat-affected zone, the length of the discoloration on the joining geometries is measured after the welding process. A smaller heat-affected zone should be aimed for as excessive heat input into the geometries can lead to distortion and damage. When evaluating the weld metal overflow, the ratio of the weld bead to the height or width of the joint geometry is measured. A welding bead that is too small indicates an inadequate connection between the two components. A welding bead that is too large indicates a melt pool that is too large and therefore an excessive change in the basic geometry. All variants in five copies are evaluated. For the heat-affected zone, the measured values are divided into quartiles and scored. The shape defects and the weld metal overflow are divided into categories on the basis of the measured values and a visual inspection. These categories describe the significance of the defects.

Destructive measurements are carried out by examining embedded, ground and polished samples of the joint parts under an optical light microscope VHX 6000® using 30× magnification. The number of pores and gas inclusions (voids) in the geometries are counted using the light microscope's software-based measuring tools (see Fig. 10). In addition, the area of the welding bead and the proportion of pores in the surface are measured. The diameter of the largest pores and voids (green) are also measured. Finally, in addition to the visual inspection, the geometries are checked for shape defects and weld metal overflows.

The metallographic examination is carried out in accordance with *DIN 5817* with the defects and irregularities defined in *DIN 6520-1*. Gas inclusions and pores (ordinal number 201), bonding defects (ordinal number 401) and cracks (ordinal number 100) are analyzed in accordance with *DIN 6520-1* [20, 21]. In the case of bonding defects, an insufficient bond between the weld metal and the base material is considered. In the case of cracks, the weld bead and the bonding points are examined for cracks. In the case of pores, a defined area of 2 × 1 mm is considered. This is placed in the center of the weld bead in the axes of the geometry and the conventional conductor. In addition to the number of pores, the percentage of pores in the total area is also evaluated. Finally, the diameter of the largest pore is considered. The individual measured values are averaged for each connection geometry and divided into quantiles.

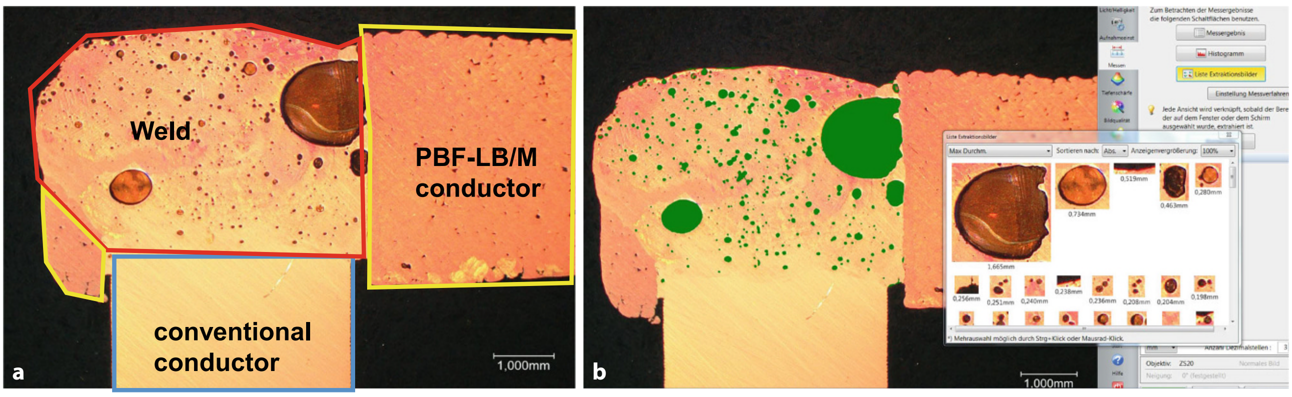

Fig. 10: Screenshot of the measurement of pores, voids and overall weld joint geometry

 © The Author(s)

3. Results

In Fig. 11, results of the design evaluation are shown exemplary for the best three design variants:

From an AM perspective, the evaluation shows the best results for geometries 17 ,13 and 16. Here, the utilization of AM design potentials to realize a form fitting, less required additional design space and small changes of cross sectional areas led to good results. Evaluation results of the industrial perspective were best for geometries 16, 17 and 1 due to high scores regarding high automation capabilites, robustness and low complexity.

In Fig. 12 the measured and calculated electrical conductivity values are shown including the standard deviation:

Here, geometries 14, 16, and 18 show the best results regarding electrical conductivity values. Geometry 14 reached 50.5 MS/m which stands for an IACS values of 87%. It should be mentioned here that a value of 54.8 MS/m was measured on the purely conventional conductor as a comparison, which corresponds to an IACS value of 94.5%.

Figure 13 shows the measured maximum temperatures during the heating investigation. Geometries 9 (110.3 °C), 16 (112.3 °C) and 4 (112.9 °C) exhibit the lowest heating. It should be noted that all geometry variants did not exceed the critical temperature of 180 °C. In a real application, however, the temperature may be higher due to an alternating voltage and the resulting alternating current losses.

In Fig. 14, the measured and calculated results of a good, medium and a bad welding are shown exemplary:

The welding evaluation results show also good scores for geometry 16. The achieved welding joint has low percentage of pores, low number of small pores, insignificant weld overflow and form error as well as a small length of the heat-affected zone. In contrast to that, geometry 5 led to a bad welding joint with high percentage and a high number of big pores. The weld overflow was evaluated as high with a strong form error as well as a long heat-affected zone.

4. Discussion

Overall, across an AM and an industrial perspective, design variant 16 was rated best. With an achieved electrical conductivity of 85.5% IACS, a maximum reached temperature of 112.3 °C, an integrated form fitting by means of a retaining bracket, a generated designated weld, a robust design in combination with a conventional conductor that does

Evaluation - AM perspective		
Rank	Geometry	Utility normalized
1	17	7,10
2	13	6,81
3	16	6,67

Evaluation - Industrial perspective		
Rank	Geometry	Utility normalized
1	16	5,68
2	17	5,54
3	1	5,52

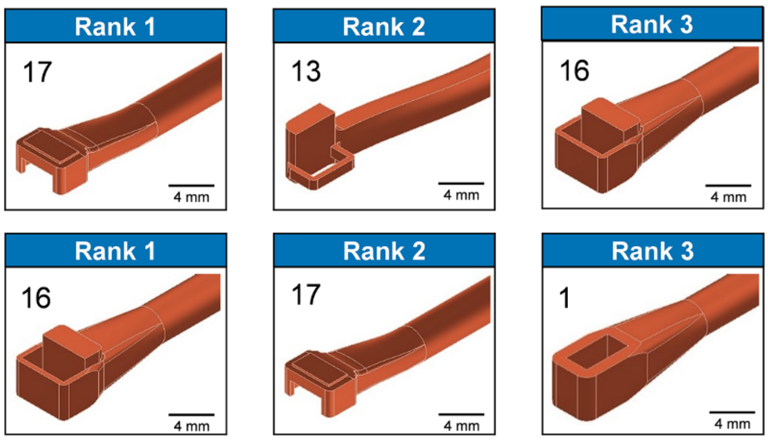

Fig. 11: Results of the utility analysis of the developed design variants. Best three variants are shown

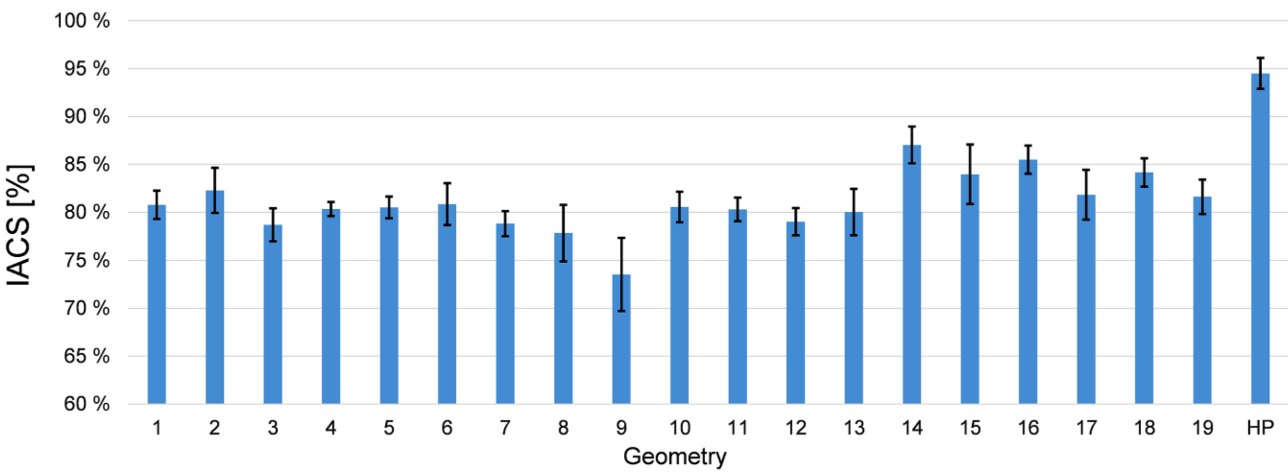

Fig. 12: Results of the calculated electrical conductivity values for each design variant and a conventional wire (HP)

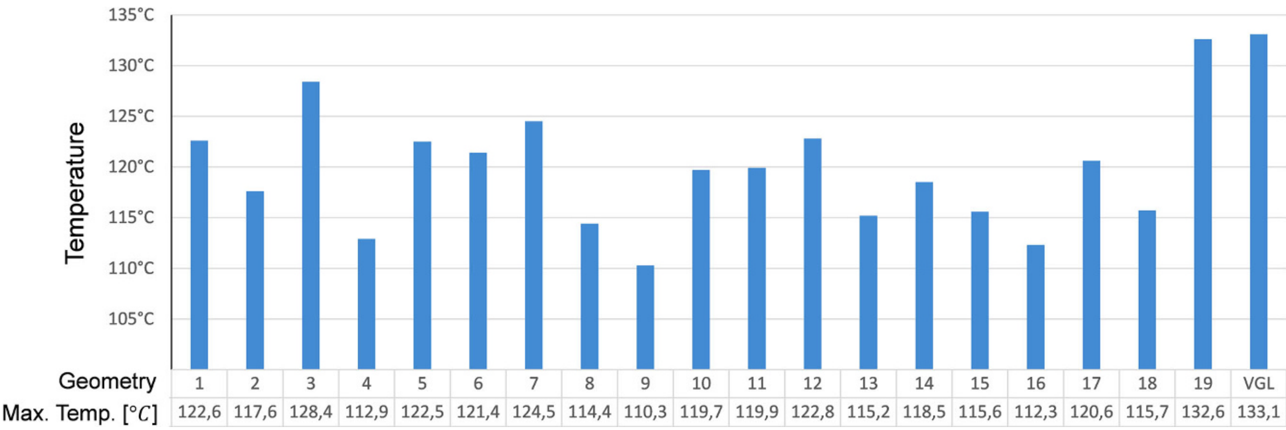

Fig. 13: Results of the temperature measurements of each welding sample and a PBF-LB/M-only sample (VGL)

			Metallographic investigation				Optical inspection			
Rank	Geo	Points	Pores [%]	Pores [nr.]	SD Poren Ø [mm]	max. Poren Ø [mm]	WO	FE	HAZ [mm]	SD HAZ
1	16	22	2,63%	10,7	0,051	0,271	insignificant	insignificant	3,80	0,74
10	10	15	4,85%	41,3	0,033	0,259	insignificant	low	4,22	0,27
19	5	2	7,85%	50,7	0,077	0,547	high	strong	6,19	1,02

SD = Standard deviation, WO = Weld overflow, FE = Form error, HAZ = Heat affected zone

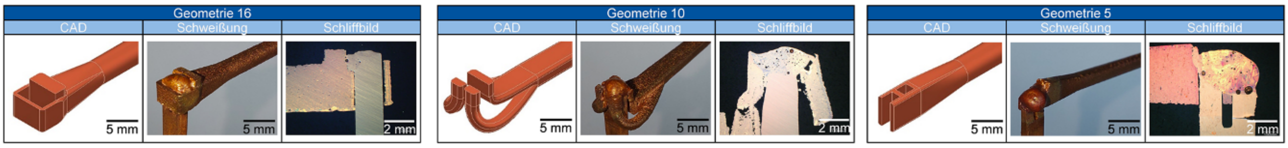

Fig. 14: Results of the welding joint investigation exemplary shown for three welding samples

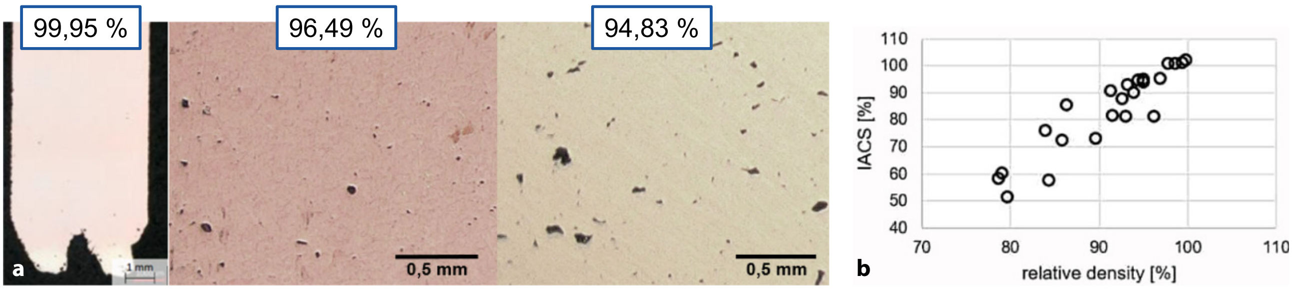

Fig. 15: Achieved relative density of pure copper samples in past studies using the applied parameter set (99.95%) with full laser power and currently achieved relative densities with less laser power (96.49%, 94.83%) (**a**) | Correlation between relative density and IACS value of pure copper AM samples (**b**) [23, 24]

not require any post-processing, the analyses and evaluations resulted in the first place. By taking advantage of AM design potentials, it was possible to integrate a form fitting design feature to create the welding joint without any additional clamping tools and without increasing the complexity much. Due to the thin-walled retaining bracket design feature, a small additional design space is needed and the change of the cross-sectional area can be kept nearly constant leading to constant electrical resistance in this area. Geometry variant 14 is the same approach, but with a smaller retaining bracket, leading to a less robust design. The third best evaluated variant is geometry 15. Here, a form and force fitting could be realized by an undersized gripping mechanism, which is split up to apply the forces from the sides. The required design space is higher compared to variants 14 and 16.

The design was discussed in particular in the context of conventional conductor pairings for the laser welding process, whereby approaches are pursued to create a form fit by attaching an additional retaining element to the welded pairing. The design of the retaining element is similar to the concept of design variant 16 in the present work [22].

When carrying out this work and generating the results, there were limiting factors, particularly with regard to electrical conductivity. The post-treated copper powder used has a reduced electrical conductivity due to the metal hydroxides applied to increase the absorption rate. According to the manufacturer, around a percentage of 91% IACS is possible here. In addition, on the PBF-LB/M system used,

 © The Author(s)

only around 80% of the set laser power could be called up, which meant that the relative density of the samples produced was lower than with full laser power. In another study, it was determined that there is a direct correlation between the relative density of copper samples and the ICAS value (Fig. 15; [23]). It is expected that the electrical conductivity values would have been higher if the maximum laser power had been available.

5. Conclusion and Outlook

By exploiting the AM design potential, a connector geometry can be created that can be joined with conventional conductors using a laser welding process and also integrates functions such as a form fit with consistent cross-sectional transitions. Even the achieved electrical conductivity of the PBF-LB/M manufactured samples was lower than expected due to the used powder and the lack of laser power, but the overall goal to develop weldable designs was reached. The process parameters of the laser welding process were based on conventional part combinations and led to first promising results. But there is potential to further optimize the parameters in future works and to develop a parameter set especially for combinations of PBF-LB/M manufactured and conventional copper parts.

Funding. The presented methodologies and results were partly researched and generated in the publicly funded project "HaPiPro[2]". In the project (duration 08/2020–02/2024), innovative and variant-flexible product and production concepts of a hairpin stator production are researched and developed. HaPiPro[2] is funded by the Ministry of Economic Affairs, Industry, Climate Protection and Energy of the State of North Rhine-Westphalia and is under the sponsorship of Projektträger Jülich (registration number EFO/0011).

Funding. Open Access funding enabled and organized by Projekt DEAL.

Conflict of interest. C. Putz, T. Grundmann and J.H. Schleifenbaum declare that they have no competing interests.

Open Access Dieser Artikel wird unter der Creative Commons Namensnennung 4.0 International Lizenz veröffentlicht, welche die Nutzung, Vervielfältigung, Bearbeitung, Verbreitung und Wiedergabe in jeglichem Medium und Format erlaubt, sofern Sie den/die ursprünglichen Autor(en) und die Quelle ordnungsgemäß nennen, einen Link zur Creative Commons Lizenz beifügen und angeben, ob Änderungen vorgenommen wurden. Die in diesem Artikel enthaltenen Bilder und sonstiges Drittmaterial unterliegen ebenfalls der genannten Creative Commons Lizenz, sofern sich aus der Abbildungslegende nichts anderes ergibt. Sofern das betreffende Material nicht unter der genannten Creative Commons Lizenz steht und die betreffende Handlung nicht nach gesetzlichen Vorschriften erlaubt ist, ist für die oben aufgeführten Weiterverwendungen des Materials die Einwilligung des jeweiligen Rechteinhabers einzuholen. Weitere Details zur Lizenz entnehmen Sie bitte der Lizenzinformation auf http://creativecommons.org/licenses/by/4.0/deed.de.

References

1. Schuhmann, D., Rockinger, C., Merkel, M., Harrison, D.K.: A study on additive manufacturing for electromobility. World Electr. Veh. J. **13**, 154 (2022). https://doi.org/10.3390/wevj13080154
2. Simpson, N. et al.: Additive manufacturing of a conformal hybrid-strand concentrated winding topology for minimal AC loss in electrical machines. In: IEEE Energy Conversion Congress and Exposition (ECCE), pp. 3844–3851. (2021) https://doi.org/10.1109/ECCE47101.2021.9595059
3. Putz, C., Reich, S., Ziegler, S.: Hybrid PBF-LB/M of pure copper for hairpin winding heads of electric traction drives. Berg Huettenmaenn Monatsh **169**, 23–30 (2024). https://doi.org/10.1007/s00501-023-01420-w
4. Putz, C., et al.: Digitale Assistenzsysteme für die effiziente Entwicklung einer neuen Produktgeneration. In: Kynast, M. (ed.) Proceedings of the 19th Rapid.Tech 3D Conference Erfurt, 9–11 May 2023. pp. 186–196. (2023) https://doi.org/10.3139/9783446479425.016
5. Werke, W.A.G.: Schweißen-von-Komponenten-aus-Kupfer-und-Kup-ferlegierungesbändern (2022). Broschüre
6. Fuessel, U., Zaehr, J., Mayer, G.: Schweißen von Kupfer und Kupferlegierungen (2009). Informationsdruck i.12
7. Liebl, S., et al.: Laser welding of copper using multi mode fiber lasers at near infrared wavelength. Phys Procedia **56**, 591–600 (2014). https://doi.org/10.1016/j.phpro.2014.08.047
8. Brunner-Schwerer, C., et al.: Laser welding of L-PBF AM components out of Inconel 718. Procedia CIRP **111**, 92–96 (2022). https://doi.org/10.1016/j.procir.2022.08.072
9. Drechsel, J., et al.: Vergleichende Untersuchungen zum Laser- und Elektronenstrahlschweißen von konventionell und additiv gefertigtem AlSi10Mg. In: 12. Mittweidaer Lasertagung, vol. 3, pp. 9–14. (2021) https://doi.org/10.48446/opus-12844
10. Ulrich, S., Rosenblatt, M., Pieper, M.: Herstellung hybrider Komponenten mittels Laserstrahlschweißen. In: 12. Mittweidaer Lasertagung, vol. 3, pp. 15–18. (2021) https://doi.org/10.48446/opus-12846
11. Feldhusen, J., Grote, K.-H.: Pahl/Beitz Konstruktionslehre: Methoden und Anwendung erfolgreicher Produktentwicklung, 8th edn. (2013). https://doi.org/10.1007/978-3-642-29569-0
12. Verein Deutscher Ingenieure: VDI 2221: Entwicklung technischer Produkte und Systeme – Modell der Produktentwicklung (2019)
13. Infinite Flex: 3D printing solutions (2024). https://infinite-flex.de/3d-printing(07/2024)
14. Hirth, U.A., et al.: Patent: Pulver zum Lasersintern und Verwendung. WO/2020/254108. Infinite Flex
15. Verein Deutscher Ingenieure: VDI 2225: Konstruktionsmethodik Technisch-wirtschaftliches Konstruieren: Blatt 3 Bewertungskriterien (1998)
16. Mühl, T.: Einführung in die elektrische Messtechnik. Springer Vieweg, Wiesbaden (2014). https://doi.org/10.1007/978-3-8348-2063-1. ISBN 978-3-8348-2063-1
17. Planing, P.: Statistik Grundlagen: 9. Konfidenzintervalle (2022)
18. United States Department of Commerce: Copper wire tables, technical report: circular of the bureau of standards no. 31, 3rd edn. (1914)
19. Deutsches Institut für Normung e.V.: Nr. 60085. Elektrische Isolierung – Thermische Bewertung und Bezeichnung (2008)
20. Deutsches Institut für Normung e.V.: Nr. 5817. Schweißen – Schmelzschweißverbindungen an Stahl, Nickel, Titan und deren Legierungen (ohne Strahlschweißen): Bewertungsgruppen von Unregelmäßigkeiten (2021)
21. Deutsches Institut für Normung e.V.: Nr. 6520-1. Schweißen und verwandte Prozesse – Einteilung von geometrischen Unregelmäßigkeiten an metallischen: Teil 1: Schmelzschweißen (2007)
22. Staeck, C.: Anfangsfestes Fügen von flachleiterbasierten Formspulen zur optimierten Schweißvorbereitung in der Hairpin-Technologie. RWTH Aachen University (2024). https://doi.org/10.18154/RWTH-2024-00373. Dissertation
23. Guschlbauer, R., Arumskog, P., Eichler, S.: Electron beam melting of pure copper—from research to industrialization. In: IVEC, pp. 89–90. (2020) https://doi.org/10.1109/IVEC45766.2020.9520506
24. Krause, F., et al.: Design, simulation and testing of additive manufactured hydrogen burners used in the EAF. Conference: 9th European Oxygen Steelmaking Conference, 6th European Conference on Clean Technologies, Aachen. (2022)

Publisher's Note. Springer Nature remains neutral with regard to jurisdictional claims in published maps and institutional affiliations.